Industrial Crops & Products 205 (2023) 117398

Contents lists available at ScienceDirect

Industrial Crops & Products

journal homepage: www.elsevier.com/locate/indcrop

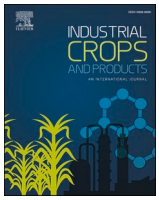

Molecular mechanism of cadmium stress response in a traditional herbal medicine *Anoectochilus roxburghii*

Shangguo Feng [a,b,d], Kaixin Zheng [a,b,d], Yadi Gao [a,b,d], Zhenhao Zhang [a,b,d], Yanyun Jin [a,b,d], Wanting Lin [a,b,d], Ruoyun Ma [a,b,d], Kailin Hou [a,b,d], Hongshan Zhang [b,c,d], Xueshuang Liang [a,b,d], Cheng Chen [c,d], Zhijing Wang [c,d], Xiaori Zhan [a,b,d], Qicai Ying [a,b,d], Huizhong Wang [a,b,d,*], Chenjia Shen [a,b,c,d,*,1]

[a] College of Life and Environmental Sciences, Hangzhou Normal University, Hangzhou 311121, China
[b] Zhejiang Provincial Key Laboratory for Genetic Improvement and Quality Control of Medicinal Plants, Hangzhou Normal University, Hangzhou 311121, China
[c] Kharkiv Institute, Hangzhou Normal University, Hangzhou 311121, China
[d] College of Pharmacy, Hangzhou Normal University, Hangzhou 311121, China

ARTICLE INFO

Keywords:
Cadmium treatment
Heavy-metal-associated P1B-type ATPase
Transcription factor

ABSTRACTS

Heavy metal toxicity is a serious constraint to orchids. *Anoectochilus* genus plants, important natural source for various active ingredients, are greatly sensitive to abiotic stress. To reveal the response mechanism of *Anoectochilus* genus to heavy metal stress, the transcriptomes of *A. roxburghii* seedlings under cadmium (Cd^{2+}) treatment were analyzed. In total, seven heavy-metal-associated P1B-type ATPase (HMA) family genes were detected in *A. roxburghii*, including two Cd^{2+} treatment inducible HMA genes (*ArHMA2* and *ArHMA5.1*). ArHMA2 and ArHMA5.1 contained classic 'E2-E2 ATPase' and 'Hydrolase' domains. Heterologous expression of *ArHMA2* and *ArHMA5.1* into the cadmium-sensitive yeast mutant strain (Δ*ycf1*) confirmed that ArHMA2 and ArHMA5.1 might play roles in the tolerance of yeast to Cd^{2+} stress. To screen their regulators, promoter sequences of *ArHMA2* and *ArHMA5.1* were cloned, and several MYB and bHLH transcription factor (TF) recognition elements were identified in their promoter regions. Furthermore, two Cd^{2+}-induced TFs, *ArMYB44.1* and *ArbHLH28*, were identified. Both in vitro and in vivo assays confirmed that ArMYB44.1 and ArbHLH28 functioned in Cd^{2+} tolerance by up-regulating the expression of *ArHMA2* and *ArHMA5.1* genes. Our data revealed novel regulatory mechanism underlying the responses to Cd^{2+} stress and contributed to the breeding of orchids with greater environmental adaptability.

1. Introduction

Heavy metals are widespread in various natural environments, such as soil, air, and water (Kintlova et al., 2017). Cadmium (Cd^{2+}), one of the common heavy metals, is considered to be no known function as nutrients or coenzyme factors. However, Cd^{2+} can be toxic to organisms in accumulated concentrations (Wu et al., 2015). Due to their chemical similarity to essential elements, heavy metals displace essential ions in enzymes and block their normal biofunctions. Cd^{2+} is potentially hazardous to human health through the food chain, and therefore, extensive research has been conducted (Ashraf et al., 2019).

Due to its mobility and persistence, Cd^{2+} can be easily absorbed by plants through a series of heavy metal transporters, even at extremely low concentrations (de Abreu-Neto et al., 2013). In plants, Cd^{2+} toxicity disturbs various physiological and secondary metabolic processes, affects growth and development, and causes leaf curling and chlorosis (Gong et al., 2023). Cd^{2+} toxicity also inhibits the absorption and subsequent transportation of nutrients, including macro elements (N, P, Mg and K) and trace elements (Mn and Zn) (Sarwar et al., 2010). Cd^{2+} excess in cells produces reactive oxygen species (ROS), resulting in oxidative stress (Tang et al., 2019). Cd^{2+} toxicity enhances the excessive accumulation of hydroxyl radical and superoxide anion by inhibiting the activities of catalase (CAT) and superoxide dismutase (SOD). Cd^{2+} induces oxidative damage, resulting in disintegration of the cell

* Corresponding authors at: College of Life and Environmental Sciences, Hangzhou Normal University, Hangzhou 311121, China.
E-mail addresses: whz62@163.com (H. Wang), shencj@hznu.edu.cn (C. Shen).
[1] Chenjia Shen will handle correspondence at all stages of refereeing and publication, also post-publication.

https://doi.org/10.1016/j.indcrop.2023.117398
Received 3 May 2023; Received in revised form 23 August 2023; Accepted 27 August 2023
Available online 6 September 2023

membrane and planned cell death (Hussain et al., 2021).

Plants evolved a series of strategies, including accumulation and transport of heavy metals, to adapt to heavy metal stresses during their growth and development process (Fasani et al., 2018). Heavy metal transporters are required for the transition of metal ions and serve as toxic ion scavengers (Williams et al., 2000). Recent advancements in molecular techniques have identified many protein families involved in metal ion transport. Heavy-metal-associated P1B-type ATPase (HMA) family is involved in pumping metals into plant cells (Hussain et al., 2004). In the model plant *Arabidopsis*, eight HMA genes were identified, including four $Zn^{2+}/Co^{2+}/Cd^{2+}/Pb^{2+}$ P1B ATPase sub-family members (AtHMA1–4) and Cu^{2+}/Ag^{1+} P1B-ATPase sub-family (AtHMA5–8) (Williams and Mills, 2005). For example, AtHMA1, a nitric oxide-responsive gene, plays an essential role in oxidative and nitrosative-mediated stress conditions (Imran et al., 2016). AtHMA2 and AtHMA4 are required for root-to-shoot Zn^{2+}/Cd^{2+} translocation (Cun et al., 2014; Wong and Cobbett, 2009). AtHMA5 is a high-affinity Cu^{2+} transporter in chloroplasts (Catty et al., 2011). However, the HMA family members in Orchidaceae have not been identified yet.

Anoectochilus roxburghii (Wall.) L. (Orchidaceae) is a perennial herb that is widely planted in Southeast Asia (Ye et al., 2017). As a valuable Chinese herbal medicine, *A. roxburghii* extracts have a specific effect on fever, inflammatory, and are frequently used to treat cystitis, nocturnal emissions and other diseases (Qiu et al., 2023). *A. roxburghii* is rich in various active ingredients, such as polysaccharides, alkaloids, and flavonoids. Kinsenoside is a pharmacologically active ingredient in *A. roxburghii* that is a bioactive glycoside component exhibiting potent anti-inflammatory and anti-oxidative abilities (Lu et al., 2022b).

The growth of orchids is confronted with various extreme environmental stresses (Li et al., 2018). Orchids, such as *Bipinnula fimbriata*, have developed various adaptation and tolerance mechanisms in a heavy metal-polluted ecosystem (Herrera et al., 2018). A number of functional genes have reportedly been involved in the responses to stress. *NPR1* and *PR1* homologs in *Cymbidium* orchids play an essential role in responses to salinity stress and viral infection (Ren et al., 2020). MSI1 plays negative regulatory roles in regulating salinity stress resistance in *Dendrobium nobile* (Cui et al., 2022). In *Phalaenopsis aphrodite*, CBF1 and ICE1 protect seedlings from cold damage through up-regulation of cold-regulated genes (Lu et al., 2022a).

Although it is an important medicinal plant, there is still limited research on the environmental adaptability of *A. roxburghii*. Revealing the expression pattern of *A. roxburghii* under heavy metal stress can help us to identify a number of candidate resistance genes. In our study, transcriptomes were used to reveal the expression responses of *A. roxburghii* seedlings to Cd^{2+} treatment. Two novel TFs, ArMYB44.1 and ArbHLH28, and their targets, *ArHMA2* and *ArHMA5.1*, were identified in *A. roxburghii*. Our data contributed to revealing the mechanism underlying the response to Cd^{2+} stress, and facilitated the breeding process of orchids with higher environmental adaptability.

2. Materials and methods

2.1. Plant materials and heavy metal treatments

Six-month-old of *A. roxburghii* seedlings were cultivated in the medicinal plants garden on the 'Cangqian' campus of Hangzhou Normal University, Hangzhou, China. The growth conditions were set as a temperature of 25 ± 1 ℃, a light cycle of 12/12 h (light/dark), and a humidity of 65–75%. For heavy metal treatment, *A. roxburghii* seedlings were placed into different groups of 6 × 6 cm glass bottles containing half-strength Hoagland solution with or without Cd^{2+}, respectively. Seedlings treated with normal half-strength Hoagland solution were used as controls. Seedlings in half-strength Hoagland solution containing 100, 200, and 300 μM of Cd^{2+} were used as treated groups. After 7 d of treatment, all seedlings were harvested for physiological parameter determination and RNA isolation. Physiological parameters under Cd^{2+} treatment were determined according to our previous published study (Feng et al., 2023).

2.2. RNA isolation and sequencing

Total leaf RNAs were isolated from *A. roxburghii* using the RNeasy Plant Mini Kit (Qiagen, Hilden, Germany) following its instruction. The contaminated genomic DNA was cleaned using an RNase-free DNase I digestion kit (TaKaRa, Dalian, China). RNA concentration was determined using a NanoDrop 2000 spectrophotometer (Thermo Scientific, Wilmington, USA), and RNA integrity was analyzed on an Agilent 2100 Bioanalyzer (Agilent, Palo Alto, USA). Each sample group has three independent biological replicates.

cDNA library construction was performed by the LC Biological Company (Hangzhou, China). cDNA libraries of different sample groups were produced using the NEBNext® Ultra™ RNA Library Prep Kit (NEB, Ipswich, MA, USA). The average insert size for the paired-end libraries was 300 bp (± 50 bp). The RNA sequencing was performed on Illumina HiSeq™ platform 4000 (LC-Bio, Hangzhou, China) to produce 100/50-bp paired/single-end small reads following the vendor's recommended protocol.

2.3. De novo assembly and annotation

Sequencing raw image data was transformed into sequence data. After quality filtering, high-quality clean reads were screened by removing low-quality sequences, such as adaptor sequences, duplicated sequences, and reads containing more than 10% unknown nucleotides. Then sequence quality was verified using FastQC (http://www.bioinformatics.babraham.ac.uk/projects/fastqc/), including the Q20, Q30 and GC-content of the clean data. *De novo* assembly was used to build different transcripts from the clean reads using Trinity software (Grabherr et al., 2011). Trinity groups transcripts into clusters based on shared sequence content. The largest transcript for each cluster was defined as a unigene.

All resulting unigenes were searched against various protein databases, including the non-redundant protein database (Nr), nucleotide database (Nt), SwissProt protein database, and Karyotic Ortholog Groups of proteins (KOG) databases using DIAMOND with a threshold of E value < 0.00001. The transcriptomes of *A. roxburghii* have been uploaded to the SRA database under accession ID PRJNA955407.

2.4. Analysis of differentially expressed genes (DEGs)

To screen the Cd^{2+} responsive genes, clean sequences were mapped onto the assembled sequence using Bowtie (version 0.12.7). To analyze gene expression levels, the normalized count number of different unigenes was calculated using the 'reads per kilobase million reads' method. Analysis of the DEGs between control and treatment groups was performed using the DESeq-R package (version 1.10.1). A corrected false discovery rate of ≤ 0.001 and $|\log_2 \text{ratio}|$ of ≥ 1 were used as the thresholds to analyze significance.

2.5. qRT-PCR analysis

Total RNAs were extracted from two groups using a Plant RNeasy Mini kit (Qiagen, Hilden, Germany). qRT-PCR was performed according to our previous study (Feng et al., 2023). *ArACTIN* gene sequence from *A. roxburghii* was used as an internal gene to calculate differences in gene expression. All the primer sequences are listed in Table S1. Three biological replications were used for expression analysis.

2.6. CDS and promoter cloning

The partial sequences of *ArHMA2*, *ArHMA5.1*, *ArbHLH28*, and *ArMYB44.1* were extracted from *A. roxburghii* transcriptome. Full-length

cDNAs of the four genes were cloned using a SMARTer RACE Kit (Clontech, Beijing, China) according to its manual. Briefly, the 5′-RACE working solution was prepared by mixing 1 μg of RNA, 1 μL of 5′ primer, 1 μL of oligonucleotide, and ddH_2O. At last, 4.5 μL of SMARTer First Strand buffer with dNTP, 0.5 μL of 100 mM dithiothreitol, 20 U of RNase inhibitor solution, and 200 U of Reverse Transcriptase were added and incubated at 42 ℃ for 90 min

High-quality genome DNAs were extracted from the *A. roxburghii* seedlings using a NuClean Plant Genomic DNA Kit (Cowin Bio., Beijing, China). The upstream promoters of *ArHMA2* and *ArHMA5.1* were cloned using a Clontech Genome Walker Kit. Briefly, genomic DNAs were digested with different restriction enzymes, and the resulting products were then added with Genome Walker adaptors. The adaptor-added sequences were treated as templates for the first-round PCR reaction. The PCR products were used as templates for the second-round PCR with nested primers. The PCR products were sequenced and used as potential promoters. The two promoter sequences are listed in Table S1.

2.7. Basic bioinformatics analysis

The transcriptomic sequences were searched against various gene databased to identify the phenylpropanoid metabolism pathway-related genes. Using the *Chrysanthemum morifolium* proteins as the query sequences, the homologous sequences of the *A. roxburghii* were searched by local BLASP program, with an *E*-value threshold of 10^{-10} (Yang et al., 2023). The expression level of the phenylpropanoid metabolism pathway-related genes were calculated according to the normalized RPKM values. The heatmap scale ranges from − 1 to + 1 on a $\log_2$ scale of expression levels.

The promoter sequences were analyzed on the PlantCARE online tool. Several important stress-related *cis*-elements, including GA-motif, MBS, TGA-element, MYC, GT1-motif, ABRE, P-box, and TCA-element, were screened. The protein sequences of each family were downloaded and used for multiple sequence alignments. Unrooted phylogenetic trees were built using MEGA6.1 with default parameters. The protein domain analysis was performed using the HMMER online program. The physical and chemical properties of ArHMA family proteins were analyzed online using ExPASy ProtParam online tool.

2.8. Method of yeast complementation

Wild-type *Saccharomyces cerevisiae* BY4741 and the mutant Δ*ycf1* were obtained from Euroscarf (Frankfurt, Germany). Transgenic cells expressing *ArHMA2* and *ArHMA5.1* were cultured on YPD solid medium with glucose. The resulting cells were then cultured in 20 mL of SD liquid medium without uracil for 48 h at 30 ℃. The pelleted cells were washed to remove liquid culture and cultured in a galactose solid medium containing 25 μM Cd^{2+}. Yeast was cultured in 20 mL of galactose solid liquid medium to an OD600 of 0.2. It was then treated with 25 μM Cd^{2+}, and the OD600 value was measured every 4-hour to record the growth curve.

The yeast cells were cultured in galactose solid medium until OD600 reached 0.2 and then treated with 25 μM Cd^{2+} for another 48 h. All the primer sequences for vector construction are listed in Table S1.

2.9. Cadmium measurement

The resulting yeast cells were harvested and washed with 5 mM $CaCl_2$ once and ddH_2O twice. Then, the clean yeast cells were dried at 80 °C and digested with 5 mL of nitric acid at 140 °C for 10 min, 200 °C for 20 min and 140 °C for 10 min. The Cd^{2+} content in yeast cells was determined using the ICP-OES 7000 system (Thermo Fisher Scientific, New York, USA). All analyses were repeated three times.

2.10. Electrophoretic mobility shift assay (EMSA)

The full-length CDSs of *ArMYB44.1* and *ArbHLH28* were cloned and inserted into the pGEX-4-T expression vector using the multiple cloning sites *BamHI/EcoRI*. The empty vector and constructs were transformed into *Escherichia coli* to produce artificial His-tagged recombinant proteins. Then, 1 mM of isopropyl-β-D-thiogalactopyranoside was added to up-regulated protein over-accumulation. The over-accumulated proteins were isolated and His-tagged purified using Clontech His60-Ni-Resin.

EMSA was performed according to our previous study (Yu et al., 2020). In brief, the MYB-binding element (MBE: CAGTTA) and bHLH-binding element (ABRE: CCCGGG) derived from the promoters of ArHMA2 and ArHMA5.1 were labeled with FAM type dye to synthesize specific probes. Sequences without a FAM dye were treated as competitors. The core probe sequences was changed to 'CCCGGG' and treated as mutation probes. The promoter sequences and probe sequences are listed in Table S1.

2.11. Dual-luciferase (Dual-LUC) reporter assay

The full-length CDSs of *ArMYB44.1* and *ArbHLH28* were inserted into the vector pBD as effectors, and the partial promoter sequences of *ArHMA2* and *ArHMA5.1* were inserted into the vector pGreenII-0800-LUC as reporters. A dual-LUC assay kit (Promega, Madison, USA) were used to determine the LUC and Renilla (REN) luciferase activities. The binding activities of ArbHLH28 to ArHMA2/ArHMA5.1 promoters and ArMYB44.1 to ArHMA2/ArHMA5.1 promoters were calculated using the LUC/REN ratios. P value < 0.05 was considered to be statistically significant. The promoter sequences are listed in Table S1.

3. Results

3.1. Physiological responses of A. roxburghii seedlings to Cd^{2+} stress

A. roxburghii seedlings were treated with 0, 100 μmol.L^{-1}, 200 μmol.L^{-1} and 300 μmol.L^{-1} $CdCl_2$ solution. Various physiological parameters, including the activities of SOD, CAT, and POD, and the contents of chlorophyll, proline, and MDA, were determined under the Cd^{2+} treatment. The activities of SOD and CAT were significantly reduced and the activities of POD were significantly induced under different concentrations of Cd^{2+} (Fig. 1a-c). However, the increase and decrease in SOD, CAT, and POD activities were not consistent with the concentration of Cd^{2+}. A reasonable explanation is that long time treatment may make the seedlings adapt to Cd^{2+} stress and result in a certain degree of recovery. The chlorophyll contents were significantly down-regulated under different concentrations of Cd^{2+} (Fig. 1d). The contents of proline and MDA were significantly up-regulated under 200 μmol.L^{-1} and 300 μmol.L^{-1} of Cd^{2+} treatments (Fig. 1e-f).

3.2. Transcriptomes of A. roxburghii seedlings under Cd^{2+} stress

Six cDNA libraries were sequenced to screen Cd^{2+}-stress responsive transcripts of *A. roxburghii*. Raw data were processed to generate 30,3765,556 clean reads, comprising about 42.62 Gb of sequence data from the all cDNA libraries (Table S2). Based on the clean reads, 178,593 transcripts (N50: 1269) with an median length of 466 bp were identified (Fig. 2a). Clustering of all transcripts resulted in 72,110 unigenes (N50: 1322) with a median length of 375 bp (Fig. 2b). The average GC contents of transcripts and unigenes are 42.11% and 42.39%, respectively (Fig. S1). The sequence lengths of the transcript and unigene are shown in Fig. 2c. In total, 142,27 transcripts and 5689 unigenes with a length of more than 2000 bp.

All assembled *A. roxburghii* unigenes were searched against various databases, producing 22,617 genes in the GO database, 17,629 genes in the KEGG database, 21,057 genes in the Pfam database, 19,098 genes in

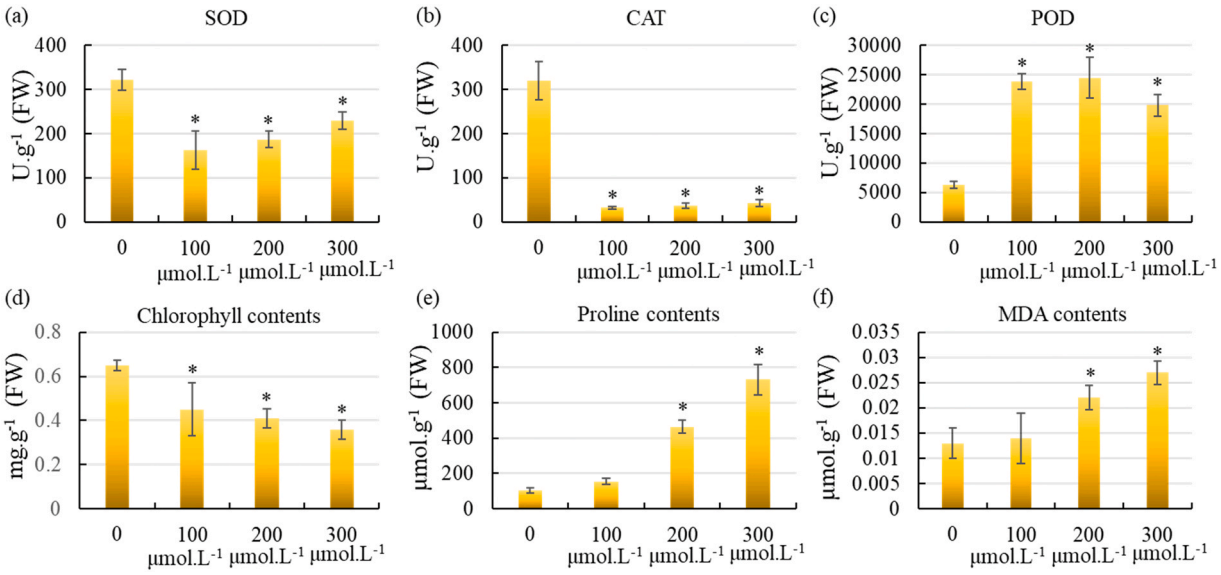

Fig. 1. Physiological parameters of *A. roxburghii* seedlings under Cd^{2+} stress. The activities of key antioxidant enzymes, such as SOD (a), CAT (b) and POD (c), under Cd treatment. Cd induced changes in chlorophyll contents (d), proline contents (e) and MDA contents (f). '*' indicates significant differences between control and Cd^{2+} treatment at $P < 0.01$. Three biological replicates were performed in each comparison group.

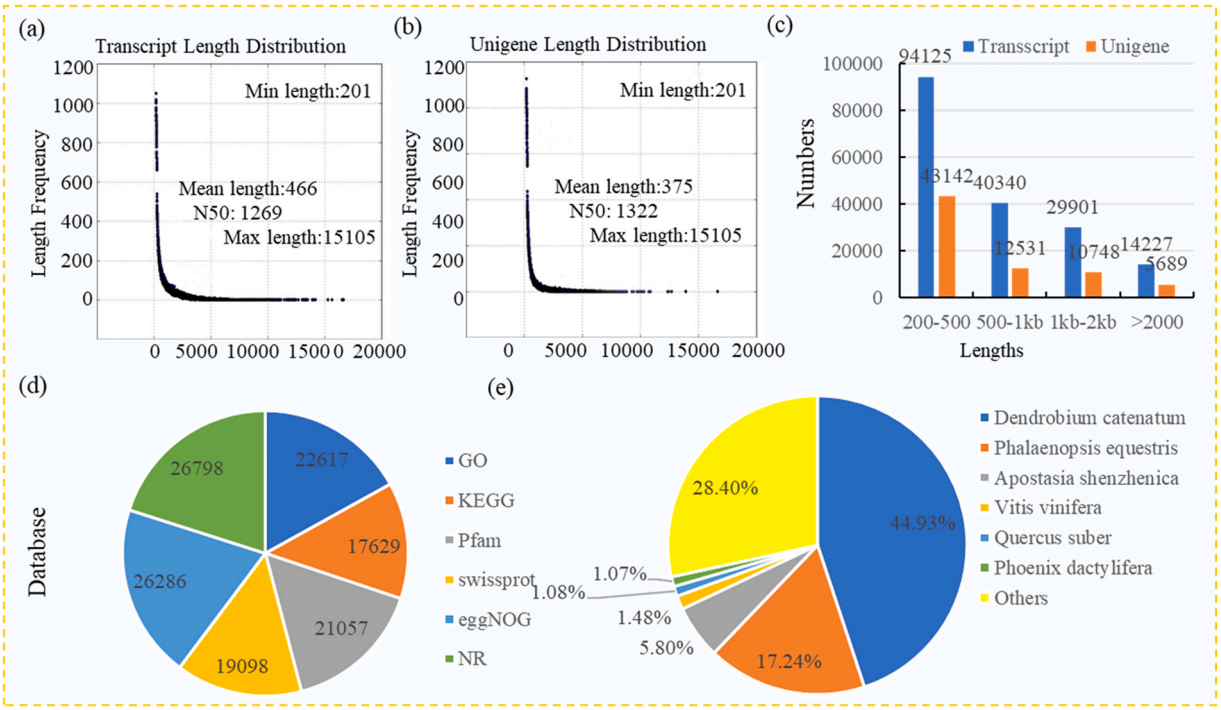

Fig. 2. Length distribution of assembled *A. roxburghii* transcripts and unigenes. (a) Transcript length distribution. (b) Unigene length distribution. (c) The length distribution of assembled transcripts and unigenes in *A. roxburghii*. (d) The number of unigenes annotated by different databases, including Nr, Swissprot, KOG, KEGG, GO and Pfam. (f) Species distribution of all annotated unigenes.

the Swissprot database, 26,286 genes in the eggNOG database, and 26,798 genes in the Nr database (Fig. 2d). The largest group of *A. roxburghii* homologous genes was identified in *Dendrobium catenatum* (44.93%), *Phalaenopsis equestris* (17.24%), *Apostasia shenzhenica* (5.8%), *Vitis vinifera* (1.48%), *Quercus suber* (1.08%), and *Phoenix dactylifera* (1.07%), indicating a close relationship among orchids (Fig. 2e).

3.3. Identification of the Cd^{2+} stress-responsive genes

To screen the Cd^{2+} responsive genes, 12,377 DEGs, including 6088 up- and 6289 down-regulated genes, were detected (Fig. 3a-b). Under Cd^{2+} treatment, the largest up-regulated genes are *Subtilisin-like protease 1.9* (SBT1.9), 14–3–3-like GF14 (GF14), and *CobN/magnesium chelatase 1* (CHLH), and the greatest down-regulated genes are *Homeobox-leucine zipper gene 19* (HOX19), *Calcineurin B-like gene 7* (CBL7), and *Phosphate translocator 2* (PT2). The GO enrichment analysis assigned most of the DEGs to at least one GO category. The most significantly enriched GO terms are 'cell wall' (GO:0005618, $P = 9.0E-12$), 'serine-type endopeptidase activity' (GO:0004252, $P = 2.9E-09$), and 'suberin biosynthetic process' (GO:0010345, $P = 3.4E-6$) (Fig. S2 and Table S3). The KEGG

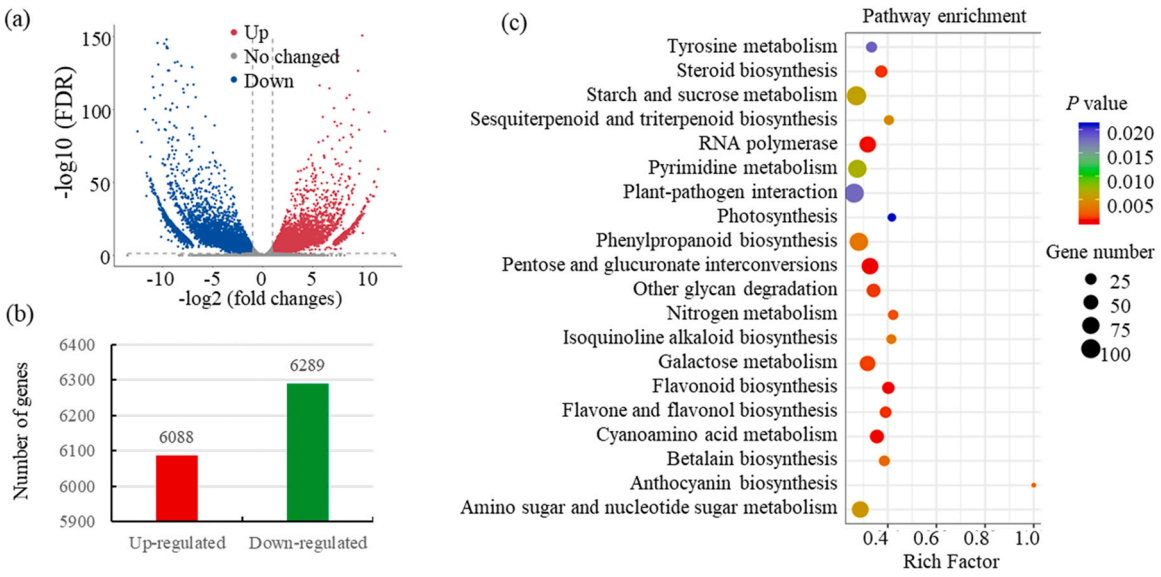

Fig. 3. Analysis of differentially expressed genes (DEGs) of *A. roxburghii* under Cd stress. (a) Volcano plots of the DEGs under Cd^{2+} stress. (b) Number of the up- and down-regulated DEGs of *A. roxburghii* under Cd^{2+} stress. (c) KEGG enrichment analysis of the DEGs under Cd^{2+} stress. Different colors indicated P values, and the circle sizes indicated DEG number.

enrichment analysis showed that genes belonging to the 'pentose and glucuronate interconversions' (map00040, $P = 1.1E-4$), 'flavonoid biosynthesis' (map00941, $P = 1.6E-4$), and 'cyanoamino acid metabolism' (map00460, $P = 2.9E-4$) were significantly changed under Cd^{2+} treatment. Besides, several other metabolism-related KEGG terms were detected, such as 'steroid biosynthesis', 'sesquiterpenoid and triterpenoid biosynthesis', 'isoquinoline alkaloid biosynthesis', 'betalain biosynthesis', and 'anthocyanin biosynthesis' (Fig. S3a and Table S4).

Several stress response- and metal ion transport-related GO terms were identified in the DEG pool. Most of the stress response-related genes were enriched in the 'peroxisome' (GO:0005777, $P = 0.027$), 'defense response' (GO:0006952, $P = 2.0E-4$), 'oxidation-reduction process' (GO:0055114, $P = 8.4E-6$), and 'oxidoreductase activity' (GO:0016491, $P = 2.7E-6$) GO terms (Fig. S3b). Most of the metal ion transport-related genes were enriched in 'transmembrane transporter activity' (GO:0022857, $P = 0.0027$), 'transmembrane transport' (GO:0055085, $P = 0.007$), 'transition metal ion binding' (GO:0046914, $P = 0.01$), 'ion transmembrane transport' (GO:0034220, $P = 0.012$), 'cellular transition metal ion homeostasis' (GO:0046916, $P = 0.018$), and 'metal ion transport' (GO:0030001, $P = 0.034$) GO terms (Fig. 3e).

3.4. Effect of Cd^{2+} stress on the phenylpropanoid metabolism pathway

Various types of phenylpropanoid compounds, such as flavonoids and chlorogenic acids, were considered to be involved in stress responses (Yang et al., 2020). Based on the *A. roxburghii* transcriptome, a number of genes encoding 10 key enzymes involved in the biosynthesis of chlorogenic acid and flavonoids were identified (Table S5). In total, eight phenylalanine ammonia-lyase (PAL) encoding genes, two trans-cinnamate 4-monooxygenase (C4M) encoding genes, 14 4-coumarate–CoA ligase (4CL) encoding genes, five chalcone synthase (CHS) encoding genes, two chalcone flavonone isomerase (CHI) encoding genes, one flavanone 3-hydroxylase (F3H) encoding gene, one flavonol synthase (FLS) encoding gene, one bifunctional dihydroflavonol 4-reductase (DFR) encoding gene, one cytochrome P450–98A2 (UGCT) encoding gene, and three hydroxy-cinnamoyl transferase (HCT) encoding genes were identified (Fig. 4a).

Under Cd^{2+} treatment, one *CHS* gene (DN45185_c2_g2), one *CHI* gene (DN46422_c2_g1), one *F3H* gene (DN37977_c3_g1), one *FLS* gene (DN33168_c0_g3), six *PAL* genes (DN37353_c0_g1, DN37353_c1_g4, DN37353_c1_g5, DN41712_c0_g3, DN42075_c0_g1, and DN42075_c0_g4), three 4CL genes (DN29538_c5_g1, DN36602_c1_g2, and DN36602_c2_g1), one *C4M* gene (DN39835_c0_g3), one *HCT* gene (DN39927_c0_g1), and one *UGCT* gene (DN31694_c0_g1) were significantly up-regulated. Meanwhile, one *DFR* gene (DN27913_c0_g1), one *PAL* gene (DN37353_c1_g2), and one *4CL* gene (DN30471_c5_g2) were significantly down-regulated by the Cd^{2+} treatment (Fig. 4b).

3.5. Analysis of the HMA family member in A. roxburghii

According to the reference sequence, seven putative HMA family members were detected in *A. roxburghii*. The full-length encoding sequences of the seven HMA genes were cloned by RACE method. The detailed information of *ArHMA* genes, such as gene names, ORF lengths, and basic parameters of their deduced peptides is listed in Table S6. A phylogenetic tree was built to analyze the relationship of HMA genes between *A. roxburghii* and model plant *Arabidopsis*. Based on the evolutionary relationship, five gene pairs were identified: ArHMA1-AtHMA1, ArHMA5.1/5.2-AtHMA5, ArHMA6-AtHMA6.1/6.2, ArHMA7-AtHMA7, and ArHMA8-AtHMA8.1/8.2 (Fig. 5a). Protein domain analysis showed that ArHMA5.1 and ArHMA6 contain three classic domains, including HMA, E1-E2 ATPase, and hydrolase. ArHMA7 and ArHMA8 only contain the hydrolase domain. ArHMA1, ArHMA2, and ArHMA5.2 contain the E1-E2 ATPase and hydrolase domains (Fig. 5b).

QRT-PCR analysis showed that *ArHMA1*, *ArHMA2*, and *ArHMA7* are specifically expressed in the leaves, *ArHMA5.2* is highly expressed in the stems, and *ArHMA8* is greatly expressed in the roots (Fig. S4). The expression of ArHMA genes under Cd^{2+} treatment was analyzed by a qRT-PCR experiment. Among the seven ArHMA family members, *ArHMA2* and *ArHMA5.1* were significantly up-regulated by Cd^{2+} treatment (Fig. 5**c**). Therefore, we focused on the two ArHMA genes in subsequent experiments.

3.6. Yeast complementation analysis of two ArHMA proteins

Cd^{2+}-sensitive *S. cerevisiae* strain *ycf1* was used to reveal the biological function of ArHMA2 and ArHMA5.1 under heavy metal stress. The full-length CDS of *ArHMA2* and *ArHMA5.1* were ectopically expressed in the control (BY4741) and mutant yeast (Δ*ycf1*) cells. The

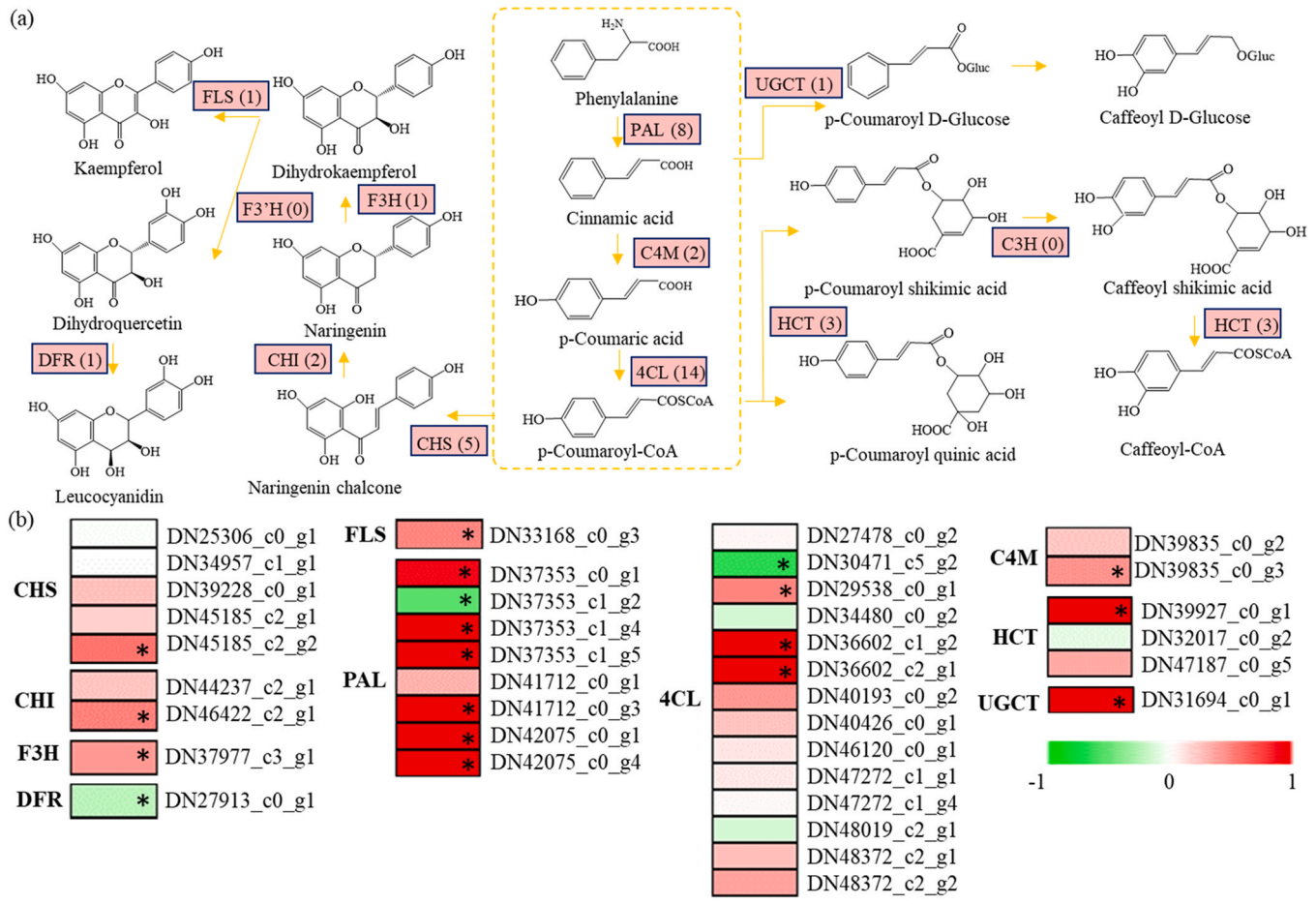

Fig. 4. Effects of Cd^{2+} stress on flavonoid and coumarin metabolism in *A. roxburghii*. (a) Overview of flavonoid and coumarin metabolic pathway in *A. roxburghii*. The numbers of encoding genes referring each enzyme were showed in brackets. Enzyme abbreviations: CHS: chalcone synthase; CHI: Chalcone–flavonone isomerase; F3H: flavanone 3-hydroxylase; DFR: dihydroflavonol 4-reductase; FLS: flavonol synthase; PAL: phenylalanine ammonia-lyase; UGCT: UDP-glucosyltransferase; 4CL: 4-coumarate–CoA ligase; C4M: trans-cinnamate 4- monooxygenase; HCT: hydroxycinnamoyl CoA quinate transferase. (b) Expression changes of genes associated with flavonoid and coumarin metabolism under Cd stress. The expression levels of each gene were showed in heatmaps. The red color indicated high expression level, green color indicated low expression level, and while color indicated median expression level. The heatmap scale ranges from − 1 to + 1 on a $\log_2$ scale normalized expression levels. '*' indicates significant differences between control and Cd^{2+} treatment at $P < 0.01$.

growth rates of BY4741 with an empty pYES2 vector during 24 h of 25 μM Cd^{2+} treatment were used as the control group. The growth rates of Δ*ycf1* cells with the empty pYES2 vector were significantly lower than those of BY4741 cells with the empty pYES2 vector. Overexpression of *ArHMA2* and *ArHMA5.1* in Δ*ycf1* cells can significantly induce their growth rates during 24 h of 25 μM Cd^{2+} treatment (Fig. 5d and Table S7). Furthermore, the Cd^{2+} contents of the above four yeast cell lines were determined. The Cd^{2+} content of BY4741 with an empty pYES2 vector was used as a control. Our data showed that the Cd^{2+} contents of Δ*ycf1* cells were significantly lower than those of BY4741 cells. Overexpression of *ArHMA2* and *ArHMA5.1* in Δ*ycf1* cells can significantly up-regulate the Cd^{2+} contents compared to the Δ*ycf1* with an empty pYES2 vector (Fig. 5e). Our data suggested that ArHMA2 and ArHMA5.1 played potential roles in the accumulation of Cd^{2+} in yeast cells.

3.7. Cloning and analysis of the promoters of ArHMA2 and ArHMA5.1

As a non-model medicinal plant, the genome sequence of *A. roxburghii* is unavailable. In our study, partial promoters of *ArHMA2* and *ArHMA5.1* were cloned and analyzed. After a two-round chromosome walking, a 1080 bp upstream promoter sequence of the *ArHMA2* gene and a 1907 bp upstream promoter sequence of the *ArHMA5.1* gene were obtained (Table S8). After *cis*-element scanning, three MBSs, one GT1-motif, one P-box, and one MYC were identified in the promoter region of *ArHMA2*. Additionally, six MYCs, four MYBs, one GT1-motif, one P-box, one TGA-element, and one ABRE were identified in the promoter region of *ArHMA5.1* (Fig. S5). Interestingly, ABRE (for bHLH binding) and MBS (for MYB binding) were detected in both the *ArHMA2* and *ArHMA5.1* promoters. Thus, we focused on the roles of MYB and bHLH family members in the regulation of *ArHMA2* and *ArHMA5.1* in the present study.

3.8. Screening of MYB and bHLH family genes responsive to Cd^{2+} stress

According to the *A. roxburghii* reference sequence, 16 ArMYB genes and 22 ArbHLH genes were identified. Two phylogenetic trees were built to reveal the relationship of MYB and bHLH family members between *A. roxburghii* and the well-studied *Arabidopsis*. All the proteins in each phylogenetic tree were grouped into three categories: defense, metabolism, and development. Several *Arabidopsis* defense-related MYB/bHLH homologous genes were predicted based on their evolutionary relationship. For the MYB family, *ArMYB44.1/44.2* (homologous genes of *AtMYB44*), *ArMYB30* (homologous gene of *AtMYB30*), and *ArMYB96* (homologous gene of *AtMYB96*) were predicted to be potential defense-related TFs (Fig. 6a). For the bHLH family, *ArbHLH11* (homologous gene of *AtbHLH11*), *ArbHLH47* (homologous gene of *AtbHLH47*), *ArbHLH28* (homologous gene of *AtbHLH28*), *ArbHLH13.1/13.2* (homologous gene

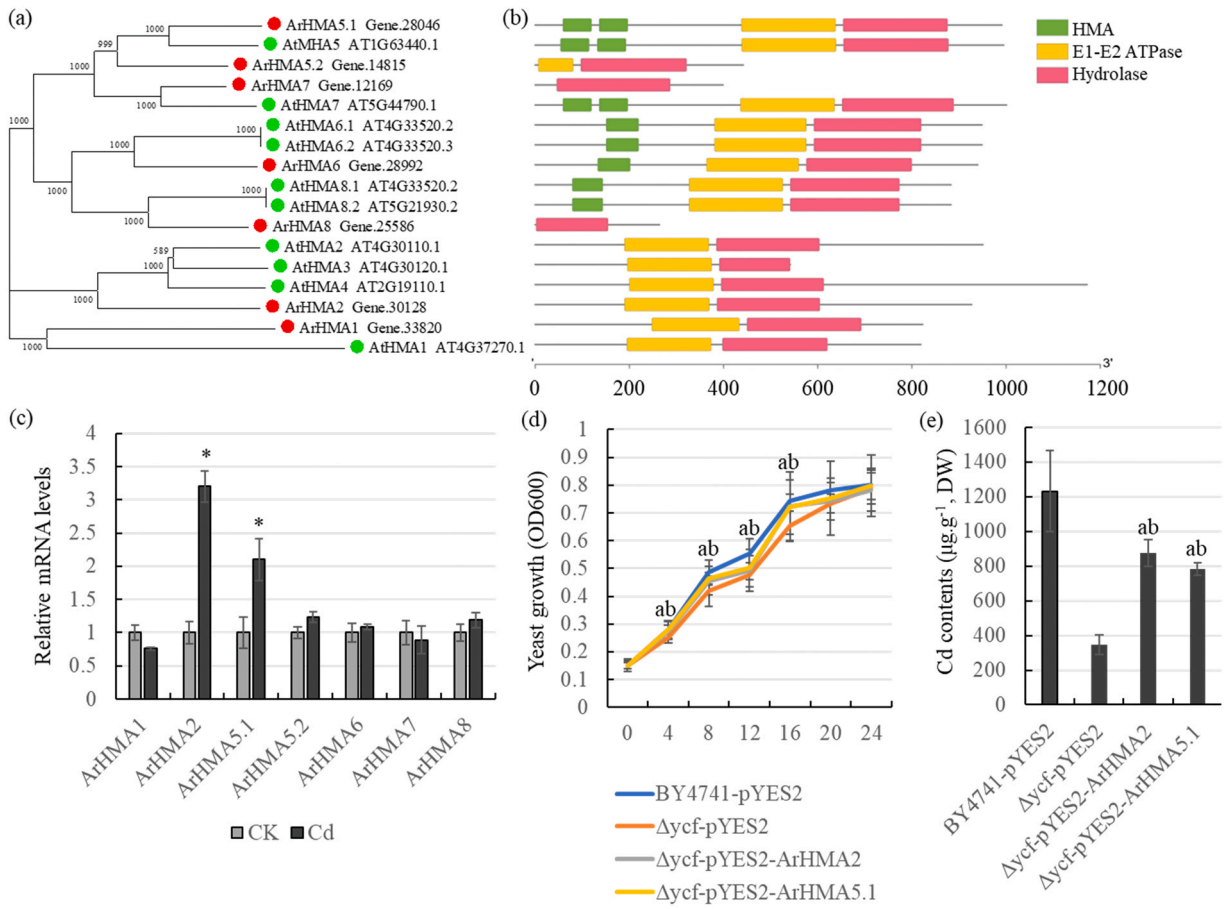

Fig. 5. Identification of *A. roxburghii* HMA proteins. (a) Evolutionary analysis of HMA proteins from *A. roxburghii* and model plant *Arabidopsis*. Red dots indicated HMA proteins from *A. roxburghii*. (b) Protein domain analysis of HMA proteins from *A. roxburghii* and *Arabidopsis*. Green boxes indicated the 'HMA' domain, yellow boxes indicated the 'E1-E2 ATPase' domain, and red boxes indicated the 'hydrolase' domain. (c) Expression analysis of ArHMA family genes under Cd treatment. '*' indicates significant differences between control and Cd treatment at $P < 0.01$. (d) The status of yeast cells at different time points during the growth process. The OD 600 of yeast cells was cultured to 0.2, $CdCl_2$ was added to make the medium concentration reach 25 μM, then samples were measured every 4 h. (e) The Cd contents in different yeast cells. Letter 'a′ indicates significant differences between control (BY4741-pYES2) and treatment groups at $P < 0.01$. Letter 'b′ indicates significant differences between control (Δ*ycf1*-pYES2) and treatment groups at $P < 0.01$. Three biological replicates were performed in each comparison group.

of *AtbHLH13*), and *ArbHLH116* (homologous gene of *AtbHLH116*) were predicted to be potential defense-related TFs (Fig. 6b).

QRT-PCR was performed to analyze the responses of potential defense-related TFs to Cd^{2+} treatment. Ten potential defense-related TF genes, including *ArMYB44.2*, *ArMYB44.1*, *ArMYB30*, *ArMYB96*, *ArbHLH28*, *ArbHLH116*, *ArbHLH13.1*, *ArbHLH13.2*, *ArbHLH11*, and *ArbHLH47*, were selected for the qRT-PCR analysis. Our data suggested that only *ArMYB44.1* and *ArbHLH28* were significantly up-regulated by the Cd^{2+} treatment (Fig. S6). The core sequences of ArMYB44.1 and ArbHLH28 were extracted from the assembled sequences. Based on the core sequences, full-length gene sequences were amplified using the RACE method. Our data indicated that ArMYB44.1 and ArbHLH28 encode putative proteins with 365 and 423 amino acid residues, respectively. Multiple sequence alignment revealed that ArMYB44.1 was a classic R2R3 type MYB family member without a common repressor domain (Fig. S7). ArbHLH28 processes classic domain that is composed of one basic region, two helix regions, and a loop region (Fig. S8).

3.9. *ArMYB44.1 and ArbHLH28 regulated the expression of ArHMA2 and ArHMA5.1*

To investigate the regulatory relationship between ArMYB44.1/ArbHLH28 and their potential targets, prokaryotic expression and affinity purification of GST-ArMYB44.1 and GST-ArbHLH28 were carried out. The binding of ArMYB44.1 and ArbHLH28 to their potential target sequences was analyzed using EMSA. Two probes surrounding the MBSs in the promoters of ArHMA2 and ArHMA5.1 were named as P-M2 (−358∼−364) and P-M5.1 (−1177∼−1183), respectively. Furthermore, two probes surrounding the ABREs in the promoters of ArHMA2 and ArHMA5.1 were named as P-A2 (−767 to 773) and P-A5.1 (−555∼−561), respectively. Our EMSA results showed that ArMYB44.1 bound directly to P-M2 and P-M5.1 probes, respectively, and ArbHLH28 bound directly to P-A2 and P-A5.1, respectively. Adding excess cold competitive probes to the reaction system significantly down-regulated the binding activities of ArMYB44.1 and ArbHLH28 proteins to their probes, while mutation probes did not affect their binding activities (Fig. 7a-d).

We performed dual-LUC reporter assays to analyze the transcriptional roles of ArMYB44.1 and ArbHLH28. The CDSs of *ArMYB44.1* and *ArbHLH28*, and the cloned promoter sequences from the *ArHMA2* and *ArHMA5.1* genes, were used to construct vectors (Fig. 7e). Our data showed that ArMYB44.1 and ArbHLH28 induced the expression level of *ArHMA2* and *ArHMA5.1*, indicating that ArMYB44.1 and ArbHLH28 functioned as two transcriptional activators (Fig. 8).

4. Discussion

Recently, breakthroughs in tissue culture and cultivation technology have led to widespread recognition of the medicinal value of

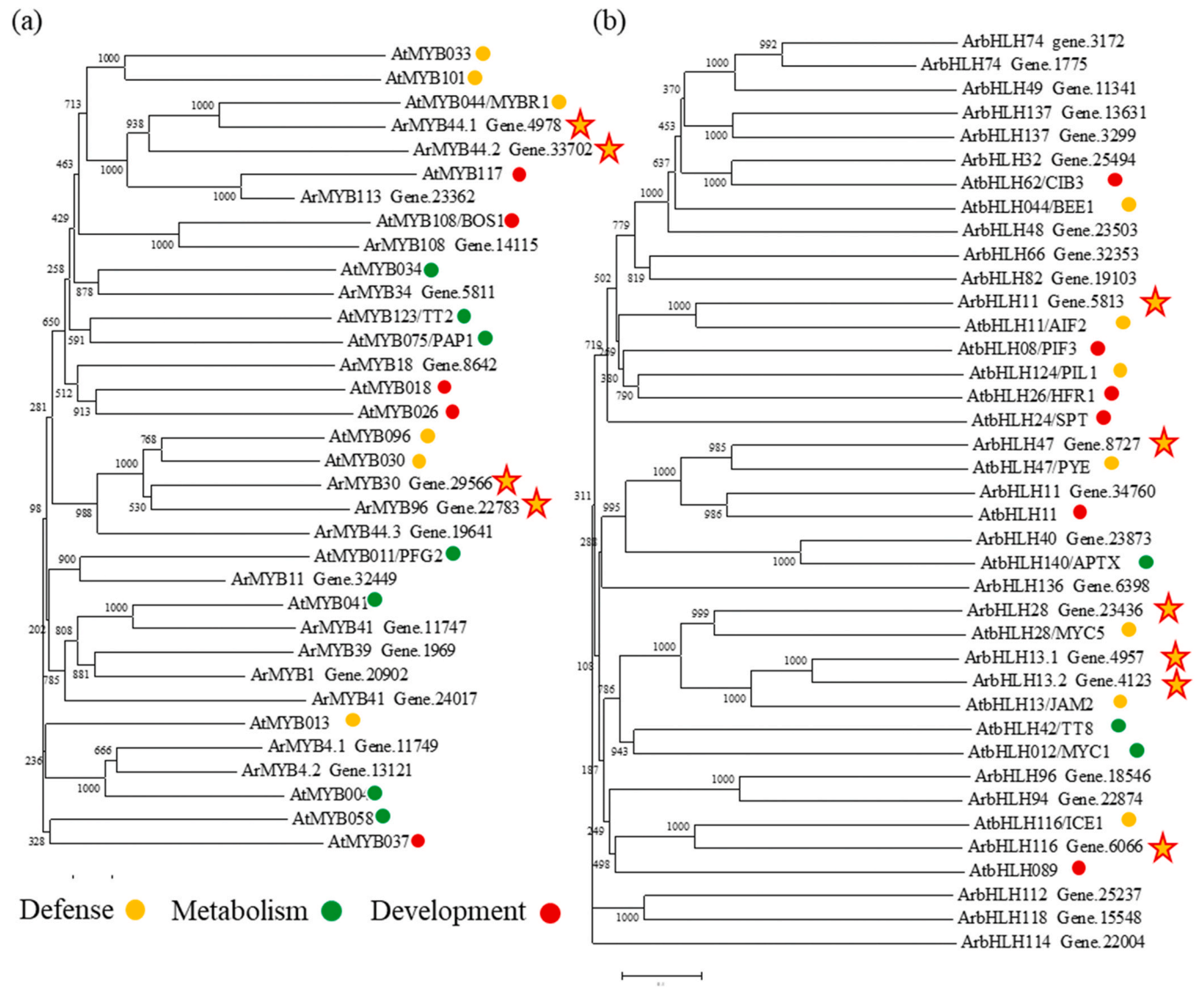

Fig. 6. Identification of the transcription factors responsive to Cd^{2+} stress. (a) Evolutionary analysis of MYB family proteins from *A. roxburghii* and model plant *Arabidopsis*. (b) Evolutionary analysis of bHLH family proteins from *A. roxburghii* and model plant *Arabidopsis*. Stars indicated TF proteins from *A. roxburghii*. Red dots indicated development-related TF proteins, green dots indicated metabolism-related TF proteins, and yellow dots indicated defense-related TF proteins. Phylogenetic tree was built using MEGA software ver. 7.1 and CLUSTALW program employing the NJ method.

A. roxburghii. Along with the wide application of *A. roxburghii* in healthcare and drinking products, its market demand continues to rise (Hong et al., 2016). Cd^{2+} is a heavy metal that does not have any physiological function and is considered to be a toxicant to human beings (Genchi et al., 2020). Cd^{2+} accumulates in plants with a long half-life period. Cd^{2+} in traditional medicine may be a risk factor for various diseases, such as renal and hepatic dysfunction, pulmonary edema, testicular damage, and damage to the adrenals and hemopoietic system (Tinkov et al., 2018). Although many researchers have focused on the active ingredients of *A. roxburghii*, there is still limited research on heavy metal-related functional gene identification (Ye et al., 2017).

High-throughput sequencing technology is an strong tool to reveal the functional genes involved in different aspects of biological processes (Feng et al., 2023; Zhan et al., 2022). To date, transcriptome and target metabolome analyses were used to investigate the genes involved in fungus-*A. roxburghii* interaction (Zhang et al., 2020a). In 2015, 11,881 DEGs between the symbiotic germinating seeds compared with the asymbiotic germinating seeds were identified by Illumina HiSeq 4000 transcriptome sequencing (Liu et al., 2015). In 2020, combined metabolome and transcriptome analyses identified 4341 *A. roxburghii* genes responsive to Mycorrhizal fungus *Ceratobasidium* sp. AR2 infection (Zhang et al., 2020b). In our study, 12,377 Cd^{2+} responsive genes were identified, suggesting that Cd^{2+} stress significantly altered the gene expression pattern of *A. roxburghii*.

Cd^{2+} toxicity severely affects plant physiological processes, including growth and metabolism (Zhan et al., 2022). Being sessile organisms, plants are frequently trapped in harsh natural environments. Trace heavy metal ions trigger various physiological and biochemical changes, which cause serious damage to plant growth and development (Singh et al., 2015). In okra (*Abelmoschus esculentus* Moench), a number of secondary metabolites, such as phenolics, flavonoids, and ascorbic acids, were significantly increased under Cd^{2+} stress (Rasheed et al., 2018). In *Pontederia cordata*, several primary metabolic pathways, such as nitrogen metabolism, starch and sucrose metabolism, and fructose and mannose metabolism, were enriched under Cd^{2+} stress (Xin et al., 2022). A previous study has pointed out that moderate Cd^{2+} treatment ($5\ mg.L^{-1}$) significantly promoted the amount of total flavonoids compared to the control (Okem et al., 2015). Flavonoids, belonging to non-enzymatic antioxidants, not only participate in regulating plant growth, but also play roles in plant protection under stress (Jiao et al.,

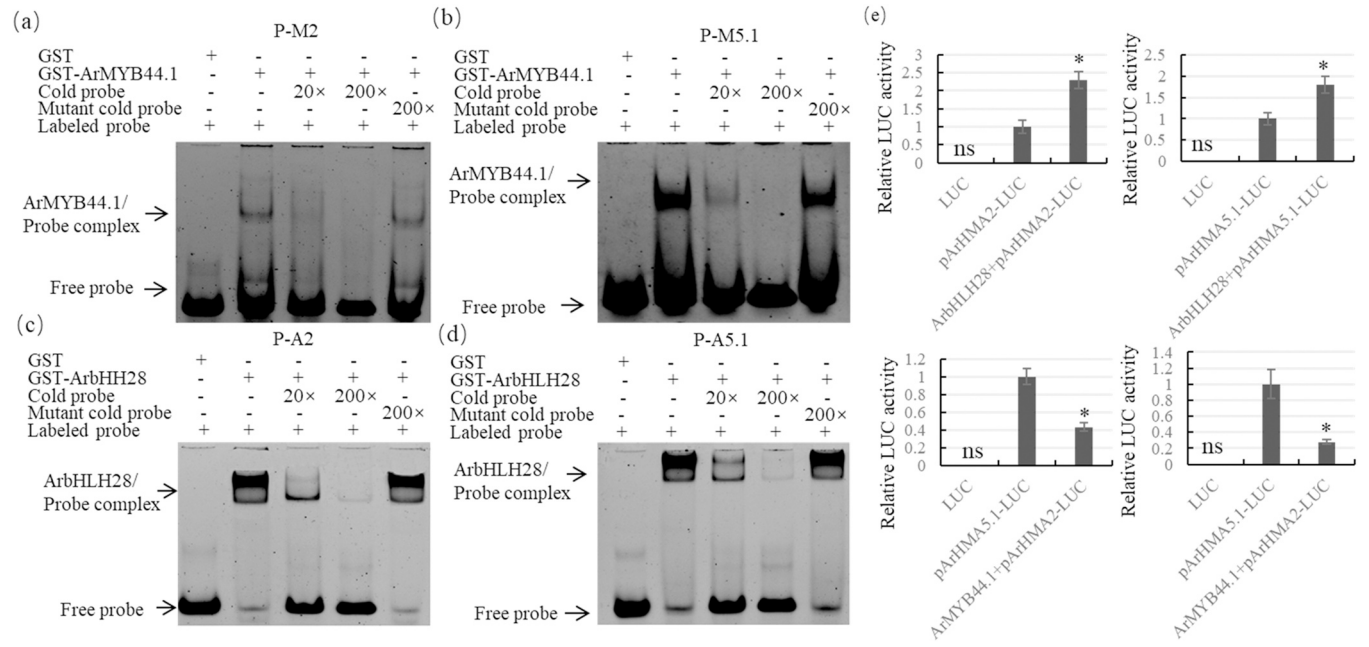

Fig. 7. The regulational functions of ArMYB44.1 and ArbHLH28 under Cd^{2+} stress. EMSA analysis of the binding of AtMYB44.1 and ArbHLH28 to their target promoter sequences. The GST only or ArMYB44.1-GST fusion proteins were incubated with probes containing the MBEs derived from the promoters of ArHMA2 (a) and ArHMA5.1 (b). The GST only or ArbHLH28-GST fusion proteins were incubated with probes containing the ABREs derived from the promoters of ArHMA2 (c) and ArHMA5.1 (d). '+' and '−' represent presence and absence, respectively, and 20 × and 200 × show increasing amounts of probes. (e) The transcriptional abilities of ArMYB44.1 and ArbHLH28 are indicated by the LUC/REN ratios. The pBD vector that produced the GAL4 DNA-BD alone was treated as negative control. Three biological repeats were used in the present study. The asterisks '*' represent significant differences between control and test groups ($P < 0.05$). Three biological replicates were performed in each comparison group.

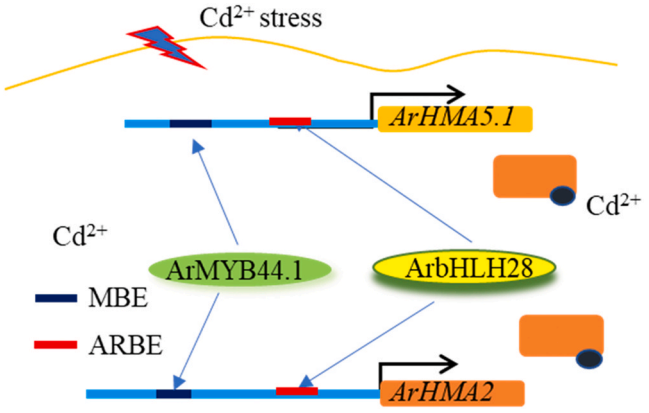

Fig. 8. A model for the role of ArMYB44.1 and ArbHLH28 in responsive to Cd^{2+} stress. ArMYB44.1 and ArbHLH28 has a significant effect on responses to Cd^{2+} stress by activating the expression of *ArHMA2 and ArHMA5.1*.

2023). In *A. roxburghii*, the content of total flavonoids was also significantly up-regulated under Cd^{2+} treatment, suggesting that the flavonoids synthesis can be up-regulated under oxidative damage. In *A. roxburghii*, the genes responsive to Cd^{2+} stress were enriched in the 'Flavonoid biosynthesis' and 'Flavone and flavonol biosynthesis' KEGG terms.

HMA protein family is responsible for plant heavy metal ion transport (Nosek et al., 2020). Recently, the HMA family has been identified in various non-model plants, such as 8 HMAs in Sedum (*Sedum plumbizincicola*), 21 HMAs in Barley (*Hordeum vulgare*), 17 HMAs in Cottonwood (*Populus trichocarpa*), and 56 HMAs in Tartary buckwheat (*Fagopyrum tataricum*) (Huang et al., 2022; Li et al., 2015; Ye et al., 2022; Zhang et al., 2021). In *A. roxburghii*, only seven HMAs were identified according to its transcriptome reference sequence. The lack of complete genome data limits the exploration of HMA genes in *A. roxburghii*. Typical HMA proteins contain an E1-E2 ATPase domain and a hydrolase domain (Li et al., 2015). In *A. roxburghii*, ArHMA7 and ArHMA8 only contain the hydrolase domain. Further experiments are needed to verify their sequence integrity.

In plants, the metal substrates of HMA proteins are not unique. For example, AtHMA2 and AtHMA4 are Zn^{2+}/Cd^{2+}-transporting ATPases and play a role in root-shoot Zn^{2+}/Cd^{2+} translocation. AtHMA5, another P-type ATPase, functions in Cu detoxification by interacting with metallochaperones, such as ATX1-like Cu chaperones (Andres-Colas et al., 2006). Interestingly, *ArHMA2* (a homologous gene of *AtHMA2*) and *ArHMA5.1* (a homologous gene of *AtHMA5*) were induced by Cd^{2+} treatment, suggesting that ArHMA2 and ArHMA5.1 might be potential multifunctional transporters. In our study, heterologous expression in yeast confirmed the role of ArHMA2 and ArHMA5.1 in the tolerance of yeast Δ*ycf1* cells to Cd^{2+} stress.

A large number of TFs, including MYB and bHLH TF family members, are involved in the regulation of corresponding heavy metal-related transcriptional processes in plants (Xie et al., 2022). For the MYB family, MYB59 in *Arabidopsis halleri*, MYB4, MYB49, and MYB59 in *Arabidopsis thaliana*, MYB16 and MYB123 in *Taxus media*, and MYB2 in *Boehmeria nivea* were reported to be involved in Cd^{2+} tolerance and accumulation (Agarwal et al., 2020; Fasani et al., 2019; Fasani et al., 2021; Feng et al., 2023; Zhu et al., 2020). For the bHLH family, overexpression of a bHLH transcription factor (ORG) enhanced heavy metal tolerance by reducing Cd^{2+} uptake and transport from roots to shoots of soybean (Xu et al., 2017). Fortunately, several MBEs (CAGTTA) and ABREs (CCCGGG) were detected in the promoter regions of *ArHMA2* and *ArHMA5.1*, suggesting that *ArHMA2* and *ArHMA5.1* are potential targets of the MYB and bHLH family members. Our study firstly uncovered the transcriptional activation of ArMYB44.1 and ArbHLH28 on *ArHMA2* and *ArHMA5.1* genes in *A. roxburghii*. As two Cd^{2+} stress-induced factors, ArMYB44.1 and ArbHLH28 rapidly respond to Cd^{2+} stress and increase the tolerance of *A. roxburghii* to Cd^{2+} stress by regulating the

expression of *ArHMA2* and *ArHMA5.1*. Our research has enriched the understanding of the environmental adaptability of medicinal plants.

5. Conclusion

We analyzed the transcriptomic profiles of *A. roxburghii* under control and Cd^{2+} stress. Two Cd^{2+} stress-inducible HMA encoding genes, *ArHMA2* and *ArHMA5.1*, were identified. Heterologous expression of *ArHMA2* and *ArHMA5.1* increased the tolerance of Δ*ycf1* cells to Cd^{2+} stress. Furthermore, two Cd^{2+} stress-induced TF genes, *ArMYB44.1* and *ArbHLH28*, were identified. ArMYB44.1 and ArbHLH28 were involved in enhancing Cd^{2+} tolerance by regulating the expression level of *ArHMA2/5.1*. Our data revealed the mechanism underlying Cd^{2+} stress and facilitated the breeding process of orchids with higher environmental adaptability.

CRediT authorship contribution statement

Shangguo Feng, Huizhong Wang and Chenjia Shen: Conceptualization. **Shangguo Feng, Zhenhao Zhang, Yadi Gao, Yanyun Jin, Kaixin Zheng, Cheng Chen and Zhijing Wang**: Data curation. **Huizhong Wang and Chenjia Shen:** Funding acquisition. **Kailin Hou, Hongshan Zhang, Qicai Ying and Xueshuang Liang**: Investigation. **Wanting Lin, Ruoyun Ma, and Xiaori Zhan**: Methodology. **Shangguo Feng**: Resources. **Chenjia Shen**: Writing – original draft. **Shangguo Feng, Huizhong Wang and Chenjia Shen**: Writing – review & editing.

Declaration of Competing Interest

The authors have no relevant financial or non-financial interests to disclose.

Data Availability

The transcriptomes of A. roxburghii have been uploaded to the SRA database under accession ID PRJNA955407.

Acknowledgements

This work was funded by National Natural Science Foundation of China (32271905 and 32270382); Zhejiang Provincial Natural Science Foundation of China under Grant No. LY23C160001, LY18C050005, LY19C150005, LY19C160001; Opening Project of Zhejiang Provincial Key Laboratory of Forest Aromatic Plants-based Healthcare Functions (2022E10008); Open Foundation of State Key Laboratory of Subtropical Silviculture, Zhejiang A & F University (KF201708); Major Increase or Decrease Program in The Central Finance Level (Grant No. 2060302); and Zhejiang Provincial Key Research and Development Project Grants (2017C02011, 2018C02030).

Appendix A. Supporting information

Supplementary data associated with this article can be found in the online version at doi:10.1016/j.indcrop.2023.117398.

References

de Abreu-Neto, J.B., Turchetto-Zolet, A.C., de Oliveira, L.F., Zanettini, M.H., Margis-Pinheiro, M., 2013. Heavy metal-associated isoprenylated plant protein (HIPP): characterization of a family of proteins exclusive to plants. FEBS J. 280, 1604–1616.

Agarwal, P., Mitra, M., Banerjee, S., Roy, S., 2020. MYB4 transcription factor, a member of R2R3-subfamily of MYB domain protein, regulates cadmium tolerance via enhanced protection against oxidative damage and increases expression of *PCS1* and *MT1C* in Arabidopsis. Plant Sci. 297, 110501.

Andres-Colas, N., Sancenon, V., Rodriguez-Navarro, S., Mayo, S., Thiele, D.J., Ecker, J.R., Puig, S., Penarrubia, L., 2006. The Arabidopsis heavy metal P-type ATPase HMA5 interacts with metallochaperones and functions in copper detoxification of roots. Plant J. 45, 225–236.

Ashraf, S., Ali, Q., Zahir, Z.A., Ashraf, S., Asghar, H.N., 2019. Phytoremediation: environmentally sustainable way for reclamation of heavy metal polluted soils. Ecotoxicol. Environ. Saf. 174, 714–727.

Catty, P., Boutigny, S., Miras, R., Joyard, J., Rolland, N., Seigneurin-Berny, D., 2011. Biochemical characterization of AtHMA6/PAA1, a chloroplast envelope Cu(I)-ATPase. J. Biol. Chem. 286, 36188–36197.

Cui, B., Huang, M., Guo, C., Li, R., Wang, Y., 2022. Cloning and expression analysis of DnMSI1 gene in orchid species *Dendrobium nobile* Lindl. Plant Signal Behav. 17, 2021649.

Cun, P., Sarrobert, C., Richaud, P., Chevalier, A., Soreau, P., Auroy, P., Gravot, A., Baltz, A., Leonhardt, N., Vavasseur, A., 2014. Modulation of Zn/Cd P(1B2)-ATPase activities in Arabidopsis impacts differently on Zn and Cd contents in shoots and seeds. Metallomics 6, 2109–2116.

Fasani, E., Manara, A., Martini, F., Furini, A., DalCorso, G., 2018. The potential of genetic engineering of plants for the remediation of soils contaminated with heavy metals. Plant Cell Environ. 41, 1201–1232.

Fasani, E., DalCorso, G., Costa, A., Zenoni, S., Furini, A., 2019. The Arabidopsis thaliana transcription factor MYB59 regulates calcium signalling during plant growth and stress response. Plant Mol. Biol. 99, 517–534.

Fasani, E., DalCorso, G., Furini, A., 2021. MYB59 transcription factor behaves differently in metallicolous and non-metallicolous populations of *Arabidopsis halleri*. Funct. Plant Biol. 48, 916–923.

Feng, S., Kailin, H., Zhang, H., Chen, C., Huang, J., Wu, Q., Zhang, Z., Gao, Y., Wu, X., Wang, H., Shen, C., 2023. Investigation of the role of TmMYB16/123 and their targets (TmMTP1/11) in the tolerance of *Taxus media* to cadmium. Tree Physiol. 43, 1009–1022.

Genchi, G., Sinicropi, M.S., Lauria, G., Carocci, A., Catalano, A., 2020. The effects of cadmium toxicity. Int J. Environ. Res Public Health 17, 3782.

Gong, Z., Duan, Y., Liu, D., Zong, Y., Zhang, D., Shi, X., Hao, X., Li, P., 2023. Physiological and transcriptome analysis of response of soybean (*Glycine max*) to cadmium stress under elevated CO(2) concentration. J. Hazard Mater. 448, 130950.

Grabherr, M.G., Haas, B.J., Yassour, M., Levin, J.Z., Thompson, D.A., Amit, I., Adiconis, X., Fan, L., Raychowdhury, R., Zeng, Q., Chen, Z., Mauceli, E., Hacohen, N., Gnirke, A., Rhind, N., di Palma, F., Birren, B.W., Nusbaum, C., Lindblad-Toh, K., Friedman, N., Regev, A., 2011. Full-length transcriptome assembly from RNA-Seq data without a reference genome. Nat. Biotechnol. 29, 644–652.

Herrera, H., Valadares, R., Oliveira, G., Fuentes, A., Almonacid, L., do Nascimento, S.V., Bashan, Y., Arriagada, C., 2018. Adaptation and tolerance mechanisms developed by mycorrhizal *Bipinnula fimbriata* plantlets (*Orchidaceae*) in a heavy metal-polluted ecosystem. Mycorrhiza 28, 651–663.

Hong, L., Shao, Q.S., Zhou, A.C., Wang, H.Z., Zhang, A.L., Xu, J.W., Huang, Y.Q., 2016. Current status and sustainable development countermeasures of *Anoectochilus roxburghii*. Zhongguo Zhong Yao Za Zhi 41, 553–558.

Huang, Q., Qiu, W., Yu, M., Li, S., Lu, Z., Zhu, Y., Kan, X., Zhuo, R., 2022. Genome-wide characterization of *Sedum plumbizincicola* HMA gene family provides functional implications in cadmium response. Plants 11, 215.

Hussain, B., Ashraf, M.N., Shafeeq Ur, R., Abbas, A., Li, J., Farooq, M., 2021. Cadmium stress in paddy fields: effects of soil conditions and remediation strategies. Sci. Total Environ. 754, 142188.

Hussain, D., Haydon, M.J., Wang, Y., Wong, E., Sherson, S.M., Young, J., Camakaris, J., Harper, J.F., Cobbett, C.S., 2004. P-type ATPase heavy metal transporters with roles in essential zinc homeostasis in Arabidopsis. Plant Cell 16, 1327–1339.

Imran, Q.M., Falak, N., Hussain, A., Mun, B.G., Sharma, A., Lee, S.U., Kim, K.M., Yun, B. W., 2016. Nitric oxide responsive heavy metal-associated gene *AtHMAD1* contributes to development and disease resistance in *Arabidopsis thaliana*. Front Plant Sci. 7, 1712.

Jiao, Z., Shi, Y., Wang, J., Wang, Z., Zhang, X., Jia, X., Du, Q., Niu, J., Liu, B., Du, R., Ji, G., Cao, J., Lv, P., 2023. Integration of transcriptome and metabolome analyses reveals sorghum roots responding to cadmium stress through regulation of the flavonoid biosynthesis pathway. Front Plant Sci. 14, 1144265.

Kintlova, M., Blavet, N., Cegan, R., Hobza, R., 2017. Transcriptome of barley under three different heavy metal stress reaction. Genom. Data 13, 15–17.

Li, D., Xu, X., Hu, X., Liu, Q., Wang, Z., Zhang, H., Wang, H., Wei, M., Wang, H., Liu, H., Li, C., 2015. Genome-wide analysis and heavy metal-induced expression profiling of the HMA gene family in *Populus trichocarpa*. Front Plant Sci. 6, 1149.

Li, J.W., Chen, X.D., Hu, X.Y., Ma, L., Zhang, S.B., 2018. Comparative physiological and proteomic analyses reveal different adaptive strategies by *Cymbidium sinense* and *C. tracyanum* to drought. Planta 247, 69–97.

Liu, S.S., Chen, J., Li, S.C., Zeng, X., Meng, Z.X., Guo, S.X., 2015. Comparative transcriptome analysis of genes involved in GA-GID1-DELLA regulatory module in symbiotic and asymbiotic seed germination of *Anoectochilus roxburghii* (Wall.) Lindl. (*Orchidaceae*). Int J. Mol. Sci. 16, 30190–30203.

Lu, C., Ye, J., Chang, Y., Mi, Z., Liu, S., Wang, D., Wang, Z., Niu, J., 2022a. Genome-wide identification and expression patterns of the SWEET gene family in *Bletilla striata* and its responses to low temperature and oxidative stress. Int. J. Mol. Sci. 23, 10057.

Lu, L., Xiong, Y., Lin, Z., Chu, X., Panayi, A.C., Hu, Y., Zhou, J., Mi, B., Liu, G., 2022b. Advances in the therapeutic application and pharmacological properties of kinsenoside against inflammation and oxidative stress-induced disorders. Front Pharm. 13, 1009550.

Nosek, M., Kaczmarczyk, A., Jedrzejczyk, R.J., Supel, P., Kaszycki, P., Miszalski, Z., 2020. Expression of genes involved in heavy metal trafficking in plants exposed to salinity stress and elevated Cd concentrations. Plants (Basel) 9, 475.

Okem, A., Stirk, W.A., Street, R.A., Southway, C., Finnie, J.F., Van Staden, J., 2015. Effects of Cd and Al stress on secondary metabolites, antioxidant and antibacterial activity of *Hypoxis hemerocallidea* Fisch. & C.A. Mey. Plant Physiol. Biochem 97, 147–155.

Qiu, Y., Song, W., Yang, Y., Zhou, G., Bai, Y., Akihisa, T., Ye, F., Feng, F., Zhang, W., Zhang, J., 2023. Isolation, structural and bioactivities of polysaccharides from *Anoectochilus roxburghii* (Wall.) Lindl.: A review. Int J. Biol. Macromol. 236, 123883.

Rasheed, R., Arslan Ashraf, M., Kamran, S., Iqbal, M., Hussain, I., 2018. Menadione sodium bisulphite mediated growth, secondary metabolism, nutrient uptake and oxidative defense in okra (*Abelmoschus esculentus* Moench) under cadmium stress. J. Hazard Mater. 360, 604–614.

Ren, R., Wei, Y., Ahmad, S., Jin, J., Gao, J., Lu, C., Zhu, G., Yang, F., 2020. Identification and characterization of NPR1 and PR1 homologs in *Cymbidium* orchids in response to multiple hormones, salinity and viral stresses. Int. J. Mol. Sci. 21, 1977.

Sarwar, N., Saifullah, Malhi, S.S., Zia, M.H., Naeem, A., Bibi, S., Farid, G., 2010. Role of mineral nutrition in minimizing cadmium accumulation by plants. J. Sci. Food Agr. 90, 925–937.

Singh, S., Parihar, P., Singh, R., Singh, V.P., Prasad, S.M., 2015. Heavy metal tolerance in plants: role of transcriptomics, proteomics, metabolomics, and ionomics. Front Plant Sci. 6, 1143.

Tang, C., Zhang, R., Hu, X., Song, J., Li, B., Ou, D., Hu, X., Zhao, Y., 2019. Exogenous spermidine elevating cadmium tolerance in *Salix matsudana* involves cadmium detoxification and antioxidant defense. Int J. Phytoremediat. 21, 305–315.

Tinkov, A.A., Filippini, T., Ajsuvakova, O.P., Skalnaya, M.G., Aaseth, J., Bjorklund, G., Gatiatulina, E.R., Popova, E.V., Nemereshina, O.N., Huang, P.T., Vinceti, M., Skalny, A.V., 2018. Cadmium and atherosclerosis: a review of toxicological mechanisms and a meta-analysis of epidemiologic studies. Environ. Res 162, 240–260.

Williams, L.E., Mills, R.F., 2005. P(1B)-ATPases–an ancient family of transition metal pumps with diverse functions in plants. Trends Plant Sci. 10, 491–502.

Williams, L.E., Pittman, J.K., Hall, J.L., 2000. Emerging mechanisms for heavy metal transport in plants. Biochim Biophys. Acta 1465, 104–126.

Wong, C.K.E., Cobbett, C.S., 2009. HMA P-type ATPases are the major mechanism for root-to-shoot Cd translocation in *Arabidopsis thaliana*. N. Phytol. 181, 71–78.

Wu, Q., Leung, J.Y., Geng, X., Chen, S., Huang, X., Li, H., Huang, Z., Zhu, L., Chen, J., Lu, Y., 2015. Heavy metal contamination of soil and water in the vicinity of an abandoned e-waste recycling site: implications for dissemination of heavy metals. Sci. Total Environ. 506–507, 217–225.

Xie, Y.F., Zhang, R.X., Qin, L.J., Song, L.L., Zhao, D.G., Xia, Z.M., 2022. Genome-wide identification and genetic characterization of the CaMYB family and its response to five types of heavy metal stress in hot pepper (*Capsicum annuum* cv. CM334). Plant Physiol. Biochem 170, 98–109.

Xin, J., Zhao, C., Li, Y., Ma, S., Tian, R., 2022. Transcriptional, secondary metabolic, and antioxidative investigations elucidate the rapid response mechanism of *Pontederia cordata* to cadmium. Ecotoxicol. Environ. Saf. 232, 113236.

Xu, Z., Liu, X., He, X., Xu, L., Huang, Y., Shao, H., Zhang, D., Tang, B., Ma, H., 2017. The soybean basic helix-loop-helix transcription factor ORG3-like Enhances cadmium tolerance via increased iron and reduced cadmium uptake and transport from roots to shoots. Front Plant Sci. 8, 1098.

Yang, Y., Guo, J., Cheng, J., Jiang, Z., Xu, M., 2020. Identification of UV-B radiation responsive microRNAs and their target genes in chrysanthemum (*Chrysanthemum morifolium* Ramat) using high-throughput sequencing. Ind. Crop Prod. 151, 112484.

Yang, Y., Liu, J., Yi, T., Li, Y., Li, M., Liu, H., Zheng, L., Chen, Z., Hao, J., Xu, M., Shen, C., 2023. Integrated mRNA and miRNA omics reveal the regulatory role of UV-B radiation in active ingredient biosynthesis of *Chrysanthemum morifolium* Ramat. Ind. Crop Prod. 197, 116657.

Ye, S., Shao, Q., Zhang, A., 2017. *Anoectochilus roxburghii*: a review of its phytochemistry, pharmacology, and clinical applications. J. Ethnopharmacol. 209, 184–202.

Ye, X., Liu, C., Yan, H., Wan, Y., Wu, Q., Wu, X., Zhao, G., Zou, L., Xiang, D., 2022. Genome-wide identification and transcriptome analysis of the heavy metal-associated (HMA) gene family in *Tartary buckwheat* and their regulatory roles under cadmium stress. Gene 847, 146884.

Yu, C., Luo, X., Zhang, C., Xu, X., Huang, J., Chen, Y., Feng, S., Zhan, X., Zhang, L., Yuan, H., Zheng, B., Wang, H., Shen, C., 2020. Tissue-specific study across the stem of *Taxus media* identifies a phloem-specific TmMYB3 involved in the transcriptional regulation of paclitaxel biosynthesis. Plant J. 103, 95–110.

Zhan, X., Chen, Z., Chen, R., Shen, C., 2022. Environmental and genetic factors involved in plant protection-associated secondary metabolite biosynthesis pathways. Front Plant Sci. 13, 877304.

Zhang, C., Yang, Q., Zhang, X., Zhang, X., Yu, T., Wu, Y., Fang, Y., Xue, D., 2021. Genome-wide identification of the HMA gene family and expression analysis under Cd stress in barley. Plants 10, 1849.

Zhang, Y., Li, Y., Guo, S., 2020a. Effects of the mycorrhizal fungus *Ceratobasidium* sp. AR2 on growth and flavonoid accumulation in *Anoectochilus roxburghii*. PeerJ 8, e8346.

Zhang, Y., Li, Y., Chen, X., Meng, Z., Guo, S., 2020b. Combined metabolome and transcriptome analyses reveal the effects of mycorrhizal fungus *Ceratobasidium* sp. AR2 on the flavonoid accumulation in *Anoectochilus roxburghii* during different growth stages. Int J. Mol. Sci. 21, 564.

Zhu, S., Shi, W., Jie, Y., Zhou, Q., Song, C., 2020. A MYB transcription factor, BnMYB2, cloned from ramie (*Boehmeria nivea*) is involved in cadmium tolerance and accumulation. PloS One 15, e0233375.